Draft version October 20, 2015
Preprint typeset using LaTeX style emulateapj v. 5/2/11

OPTICAL I-BAND LINEAR POLARIMETRY OF THE MAGNETAR 4U 0142+61 WITH SUBARU

Zhongxiang Wang[1], Yasuyuki T. Tanaka[2], Chen Wang[3], Koji S. Kawabata[2], Yasushi Fukazawa[4], Ryosuke Itoh[4], Anestis Tziamtzis[1]

Draft version October 20, 2015

ABSTRACT

Magnetars are known to have optical and/or infrared emission, but the origin of the emission is not well understood. In order to fully study their emission properties, we have carried out for the first time optical linear polarimetry of the magnetar 4U 0142+61, which has been determined from different observations to have a complicated broad-band spectrum over optical and infrared wavelengths. From our I-band imaging polarimetric observation, conducted with the 8.2-m Subaru telescope, we determine the degree of linear polarization $P = 1.0\pm3.4\%$, or $P \leq 5.6\%$ (90% confidence level). Considering models suggested for optical emission from magnetars, we discuss the implications of our result. The upper limit measurement indicates that different from radio pulsars, magnetars probably would not have strongly polarized optical emission if the emission arises from their magnetosphere as suggested.

Subject headings: X-rays: stars — stars: neutron — pulsars: individual (4U0142+61) — polarization

1. INTRODUCTION

It is currently accepted that magnetars are highly magnetized neutron stars whose dipole magnetic field reaches $\sim 10^{14}$–10^{15} G, implied by their slow spin periods of 2–12 s and rapid spin-down rates of $10^{-12} - 10^{-10}$ s s^{-1} (see reviews, e.g., given by Woods & Thompson 2006; Kaspi 2007; Mereghetti 2013; but see Rea et al. 2010, 2012 for two low magnetic field magnetar cases recently discovered). Neutron stars which have traditionally been classified as anomalous X-ray pulsars (AXPs) or soft Gamma-ray repeaters (SGRs) belong to this magnetar class, and over 20 magnetars have been identified up to now (Olausen & Kaspi 2014). Their bright X-ray luminosities cannot be explained by rotational energy loss rates and hence the energy source is considered to be provided by the decay of their ultra-strong magnetic fields. AXPs and SGRs are well known to show a variety of high-energy phenomena (e.g., Woods & Thompson 2006; Kaspi 2007) including the exceptionally bright 'giant flares' whose peak luminosity amounts to $\sim 10^{46}$ erg s^{-1} (e.g., Hurley et al. 1999; Terasawa et al. 2005; Tanaka et al. 2007).

In addition to these intensive studies at X-ray energies, magnetars have been subjected to multi-wavelength follow-up observations in radio, optical, and infrared (IR) bands. Among the magnetars identified so far, the AXP 4U 0142+61 is the best studied magnetar at optical and IR wavelengths due to its relatively short distance (distance $d \simeq 3.6$ kpc) and low extinction ($A_V \simeq 3.5$; Durant & van Kerkwijk 2006a,b). An optical counterpart was first discovered by Hulleman et al. (2000) from 4U 0142+61. The optical flux was higher than the Rayleigh-Jeans tail of the blackbody component seen in X-ray band, requiring another emission mechanism. Subsequently, Kern & Martin (2002) found that the optical emission is pulsed at its spin period and that the pulsed fraction is $\sim$27%, which is higher than 4%–14% observed in its X-ray emission (Gonzalez et al. 2010). A very faint near-IR counterpart was also identified by Hulleman et al. (2004), and then *Spitzer Space Telescope* detected mid-IR emission from 4U 0142+61 (Wang, Chakrabarty, & Kaplan 2006).

Importantly, Wang et al. (2006) found that two different emission components are needed to explain the combined optical and IR spectral energy distribution (SED). Namely, the thermal blackbody-like component, possibly emitted from a debris disk around the pulsar, is dominant over the 2.2–8 μm range, while another power-law like component (represented by $F_\nu \propto \nu^{0.3}$) can account for the residual emission in the optical VRI and near-IR J bands (Wang et al. 2006). Follow-up *Spitzer* mid-IR spectroscopy and 24 μm imaging of the AXP were consistent with the interpretation of a debris disk for the IR emission (Wang et al. 2008). However, the origin of the optical power-law emission is still unclear, although it would probably arise from the magnetosphere because the emission is relatively highly pulsed.

In order to shed new light on the optical emission mechanism of magnetars, we have carried out polarimetric observations for the nearest and least absorbed magnetar 4U 0142+61 using the Subaru 8.2-m telescope. In Wang, Tanaka, & Zhong (2012), we have reported a 4.3% upper limit (90% confidence level) on the degree of circular polarization in I-band emission from the source. In this paper we present the result from our linear polarimetry of the source at I-band.

2. OBSERVATION AND DATA REDUCTION

We carried out linear imaging polarimetry of 4U 0142+61 at I-band with the 8.2-m Subaru Telescope on 2013 December 22–23. Two first half of the telescope time in each night were awarded to us by the National Astronomical Observatory of Japan. Due to high humidity in the first night, only three hours of data were taken. For the second night, full five hours of the telescope time

[1] Shanghai Astronomical Observatory, Chinese Academy of Sciences, 80 Nandan Road, Shanghai 200030, China
[2] Hiroshima Astrophysical Science Center, Hiroshima University, Higashi-Hiroshima, Hiroshima 739-8526, Japan
[3] National Astronomical Observatories, Chinese Academy of Sciences, A20 Datun Road, Beijing 100012, China
[4] Department of Physical Sciences, Hiroshima University, Higashi-Hiroshima, Hiroshima 739-8526, Japan

were used.

The Faint Object Camera and Spectrograph (FOCAS; Kashikawa et al. 2002) was used for the polarimetric observation. In this mode, a Wollaston prism and a half-wave retarder are inserted to the collimated beam. An incident beam is splited by the Wollaston prism into two orthogonally polarized beams, one ordinary (o-beam) and the other extraordinary (e-beam). To avoid blending of the two beams, a standard focal mask has to be used. In order to measure the degree of linear polarization and the position angle of polarization in the celestial plane, one set of four exposures of a target with the half-wave plate at four position angles, $0\overset{\circ}{.}0$, $45\overset{\circ}{.}0$, $22\overset{\circ}{.}5$, and $67\overset{\circ}{.}5$, are required. The FOCAS detector was two fully-depleted-type 2k×4k CCDs, the pixel scale of which was $0\overset{''}{.}104\,\mathrm{pixel}^{-1}$. We 2×2 binned the detector for our observation.

In our observation, each set of four exposures were taken by setting the half-wave plate at the four position angles alternately. In order to avoid possible sever saturation caused by bright stars, the time of each exposure was 2 min. Between the sets of the exposures, the telescope was five-point dithered to avoid bad pixels on the CCDs and to help remove cosmic ray hits during the data reduction. In total, in the first and second night we obtained 19 sets and 32 sets of the exposures, respectively. The observing conditions were unfortunately mediocre comparing to what we wished ($0\overset{''}{.}5$ seeing would be ideal). The average seeing was approximately $0\overset{''}{.}80$ in the first night and $0\overset{''}{.}86$ in the second night.

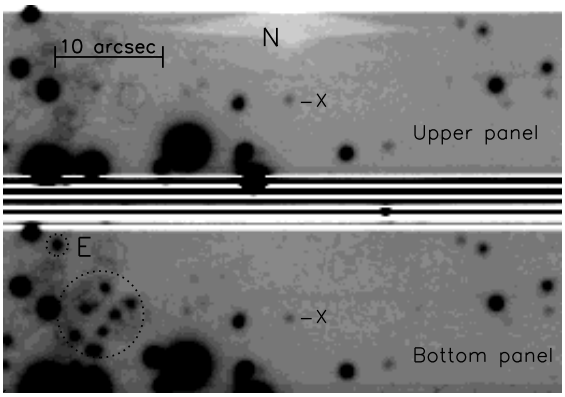

FIG. 1.— Subaru/FOCAS linear polarization image of the 4U 0142+61 field at I-band. The two polarized beams were recorded at the upper and bottom panels, in which the AXP is indicated by X. Several ghost stars, marked by dotted circles, are present in the bottom panel.

In order to determine the zero point of the position angle of polarization in the celestial plane, the standard star BD+64d106, which has strongly polarized emission, was observed.

We used the IRAF packages for data reduction. The images were bias subtracted and flat fielded. Dome flats at the four position angles of the half-wave plate were taken and used for flat fielding respectively. For our target, the images made at each angle were then combined into one final image of the target field by positionally calibrating them to a reference image. In the first night at the position angle of $45\overset{\circ}{.}0$, the target position in one image was contaminated by a cosmic ray hit, and the image was not included in image combining. In total the on-source exposure times at each position angle is 38 min (36 min for the position angle of $45\overset{\circ}{.}0$) and 64 min in the first and second night, respectively. Because of the faintness of the target and mediocre seeing during our observations, the signal-to-noise ratios of the target in each night's images are not sufficiently high. We therefore combined all the data of the two nights and made a set of four images of the target field at the four position angles respectively. A target-field image, made by combing all the images, is shown in Figure 1.

For the standard star, aperture photometry was performed and the o-beam and e-beam brightnesses at each position angle were obtained. For the target, because of its faintness, we used the point spread function (PSF) photometry tasks from IRAF's DAOPHOT package to measure its brightnesses. We also derived aperture corrections by using 8 in-field, relatively bright stars (brightest stars in the field were saturated). A radius of 10.0 pixels ($\simeq 2\overset{''}{.}1$) was used for aperture photometry of these bright stars. The uncertainties on the corrections are negligible, as they are much smaller than those from photometry of the target. These magnitude measurements and uncertainties are given in Table 1.

3. RESULTS

The degree of linear polarization P is calculated from

$$P = \sqrt{Q^2 + U^2}\ , \tag{1}$$

where Q and U are Stokes parameters. They are determined from

$$Q = \frac{1-a_1}{1+a_1},\quad U = \frac{1-a_2}{1+a_2}\ ,$$

where

$$a_1 = \sqrt{\frac{\kappa_{0\overset{\circ}{.}0}}{\kappa_{45\overset{\circ}{.}0}}},\quad a_2 = \sqrt{\frac{\kappa_{22\overset{\circ}{.}5}}{\kappa_{67\overset{\circ}{.}5}}}\ .$$

Here $\kappa = I_e/I_o$, the ratio of the intensity I of the target in the e-beam and o-beam frames at each of the four position angles of the half-wave plate. The position angle ψ of linear polarization is determined from

$$\psi = \frac{1}{2}\arctan(\frac{U}{Q})\ . \tag{2}$$

Then from standard propagation of uncertainty, where a first-order Taylor series expansion is used and the variables in the functions are assumed to be independent, the uncertainties on P and ψ can be calculated from those on intensity measurments (see, e.g., Kawabata et al. 1999).

Using the formulae given above, we first checked the polarization measurements for the standard star. From the intensity measurements, we found $P = 4.710 \pm 0.046\%$ ($Q = 2.325 \pm 0.046\%$, $U = -4.096 \pm 0.046\%$) at I-band, which is consistent with the reported value $4.696\pm0.052\%$ (Schmidt, Elston, & Lupie 1992). Therefore no instrumental correction to the polarization measurement was needed. The position angle ψ' in the instrumental coordinate (cf. Equation (2)) was found to be $\psi' = -30\overset{\circ}{.}21 \pm 0\overset{\circ}{.}28$. Comparing it to the reported value $\psi = 96\overset{\circ}{.}89 \pm 0\overset{\circ}{.}32$ (Schmidt et al. 1992), which is the position angle in the celetial plane, the correction δ was determined to be $\delta = \psi' - \psi = -127\overset{\circ}{.}10 \pm 0\overset{\circ}{.}43$.

We then calculated the Stokes parameters and degree of linear polarization for 4U 0142+61, and found $Q = -0.97 \pm 3.40\%$, $U = -0.21 \pm 3.31\%$, and $P = 1.0 \pm 3.4\%$. Since the uncertainty dominates, a 90% confidence level constraint on the degree of linear polarization was derived. The upper limit is 5.6%. In addition, also due to the large uncertainties on U and Q, $\psi = \psi' - \delta = 43^\circ \pm 96^\circ$ (where $\psi' = -83.^\circ 9$), which provides no useful information.

4. DISCUSSION

Neutron stars are known to generally have faint optical emission, either the Rayleigh-Jeans tail of high-temperature thermal surface emission or nonthermal emission arising from their magnetospheres. Optical (or near-IR) fluxes of magnetars lie above the spectra extrapolated from their blackbody-like X-ray components (e.g., Hulleman et al. 2000; Mereghetti 2013), which excludes the former case for magnetars. For the latter, polarized emission is expected and actually is observed in optical emission from radio pulsars (e.g., Słowikowska et al. 2009). While the current emission models, such as the polar cap, outer gap, two-pole caustic, and striped pulsar wind (see the detailed discussion in Słowikowska et al. 2009 and references therein), which involve radiation mechanisms including curvature, synchrotron, or inverse Compton scattering radiation, can not fully explain the well-studied Crab pulsar case, 5–10% phase-averaged linear polarization is detected in optical emission from several close or young radio pulsars (e.g., the Crab pulsar, Słowikowska et al. 2009; Moran et al. 2013; B0540−69, Middleditch et al. 1987; Lundqvist et al. 2011; the Vela pulsar, Mignani et al. 2007; Moran et al. 2014; B0656+14, Kern et al. 2003; Mignani et al. 2015; B1509−58, Wagner & Seifert 2000). The polarization upper limit of 5.6% we have obtained suggests, while marginally, a different emission mechanism from that considered in radio pulsars and thus supports a class of their own for magnetars.

Considering the surface magnetic fields of $B \sim 10^{15}$ G for magnetars, Eichler et al. (2002) have suggested that optical emission from them could be similar to radio emission from radio pulsars, i.e., due to synchrotron radiation from electron/positron pairs. In this scenario, strong linear polarization should be seen, since pulsars' radio emission is known to have the degrees of linear polarization (phase-averaged) in a range of from 10% to as high as 100% (e.g., Gould & Lyne 1998; Weltevrede & Johnston 2008; Han et al. 2009). Additionally, Beloborodov & Thompson (2007) have suggested ion cyclotron emission or curvature emission by electron/positron pairs as two possible mechanisms for magnetars' optical emission. For the both mechanisms, certain degree of linear polarization might be expected. Our measurement suggests zero or low linear polarization in optical emission, not supporting the scenarios.

However, the propagation effects in a magnetosphere may cause a strong depolarization of optical emission. The natural wave modes of optical wave in the pulsar magnetosphere are usually two orthogonal linearly polarized modes: the ordinary mode polarized in $\vec{k} - \vec{B}$ plane and the extraordinary mode perpendicular to that plane. The adiabatic evolution condition of the two linear modes is (see details in Wang, Lai, & Han 2010)

$$\Gamma_{\rm ad} = \left| \frac{\Delta k}{2\phi'_B} \right| \simeq 4 \times 10^{-5} \eta_3 \gamma_3 B_5^3 \nu_{15}^{-4} \gg 1. \quad (3)$$

Here $\eta = N/N_{\rm GJ}$ is the multiplicity, $\eta_3 = \eta/10^3$, $\gamma_3 = \gamma/10^3$ with γ the Lorentz factor of the streaming plasma, $B_5 = B/10^5$G and $\nu_{15} = \nu/10^{15}$Hz are the magnetic field strength and wave frequency. Note that we reasonably suppose $\phi'_B \sim 1/r_{\rm lc}$ ($r_{\rm lc}$ is the light cylinder radius). Assuming a dipole, the magnetic field strength can be written as

$$B = B_{*15}(r/R_*)^{-3}\,{\rm G} = 9.2 B_{*15} P_{10{\rm s}}^{-3} (r/r_{\rm lc})^{-3}\,{\rm G}, \quad (4)$$

where B_* is the surface magnetic field, $B_{*15} = B/10^{15}\,{\rm G}$, R_* the neutron star radius, and we set $R_* = 10\,{\rm km}$, $P_{10{\rm s}} = P/10{\rm s}$. For $r \gtrsim 0.015 r_{\rm lc} (\eta_3 \gamma_3 \nu_{15}^{-4})^{1/9} B_{*15}^{1/3} P_{10{\rm s}}^{-1}$, we have $|\Gamma_{\rm ad}| \ll 1$. Thus if it is in the outer magnetosphere where magnetar optical emission is generated, the mode evolution would be usually non-adiabatic, implying that the polarization direction almost does not change when propagating through the magnetosphere.

Considering the emission of a relativistic particle accelerated along the magnetic field direction, the initial polarization state should be the pure ordinary mode ($\vec{E} \parallel \vec{B}_\perp$) in each direction of the $1/\gamma$ emission cone. The polarization percentage of the combined wave of the cone obviously equals to zero at the emission point. As pointed by Cheng & Ruderman (1979), the polarization directions of the cone could be aligned by adiabatic walking after propagating a distance, which gives a very high polarization percentage such as in radio emission. However, if the optical emission comes from the outer magnetosphere, adiabatic walking would not occur since the mode evolution is non-adiabatic. The final polarization degree should be close to zero in this case. In this emission model, if the emission region extends to inner magnetosphere where mode evolution is adiabatic, partial polarization are expected, which may be the case of the Crab pulsar. For 4U 0142+61, the optical emission region could be higher so that the mode evolution is purely non-adiabatic everywhere, and the final polarization degree is close to zero.

Even the initial emission at each height is highly polarized for some other mechanisms, the total emission from the whole magnetosphere could also be depolarized due to the aberration/retardation effect. The observed emission at one phase may come from different magnetic field curve planes where the local polarization directions are different. Different from the radio band, pulsar optical emission may extend from the inner magnetosphere to light cylinder radius, such as the whole slot gap and outer gap region, which makes the depolarization due to the aberration/retardation effect much stronger. The detailed depolarization degree depends on the emission geometry in a magnetosphere. We also note that possible precession of 4U 0142+61 with a period of ∼15 hours was reported (Makishima et al. 2014), although it was not confirmed by NuSTAR observations (Tendulkar et al. 2015). This precession could cause the polarization degree to be further averaged down in our 3 and 5 hours observations.

In addition to the pulsar magnetospheric origin con-

sidered above, optical I-band emission from 4U 0142+61 could have other origin. For example, part of it (the non-pulsed component) could arise from the debris disk around the magnetar. In a recently re-proposed model for magnetars (Malheiro et al. 2012; following the pioneering work by Morini et al. 1988 and Paczynski 1990), they are suggested to be massive, highly magnetized white dwarfs with emission powered by their rotational energy (similar to pulsars). The optical and IR SED of 4U 0142+61 then might be explained by the thermal surface emission from a massive white dwarf plus that from a surrounding disk (for details, see Rueda et al. 2013). For these possibilities, low linear polarization (at most a few percent) would be expected, since the central star's emission can significantly lower the polarization level in optical light from a debris disk system (although emission from a debris disk may have high polarization; e.g., García & Gómez 2015), or thermal surface emission from a star cannot be highly polarized (e.g., Cheng et al. 1988). Our constraint on the linear polarization is actually consistent with these possibilities.

Our Subaru polarimetry likely represents the best effort for measuring polarization in optical light from 4U 0142+61 or the known magnetars in general, since they do not have detectable optical emission or are extremely faint (Olausen & Kaspi 2014). However, it would be interesting to carry out such observations when they, particularly 4U 0142+61, are in an outburst. The comparison would provide further information for our understanding of magnetars' emission mechanisms and related properties. In the future, polarimetry with an extremely large telescope, such as the Thirty-Meter Telescope, would certainly help our understanding by obtaining a much tight constraint or a measurement in a much shorter observation. The result would possibly help determine the emission mechanism at optical bands for magnetars and even identify the true nature of magnetars.

This paper is based on data collected at Subaru Telescope, which is operated by the National Astronomical Observatory of Japan.

We thank the anonymous referee for helpful suggestions and Takashi Hattori for taking the data for us. This research was supported in part by the National Natural Science Foundation of China (11373055) and the Strategic Priority Research Program "The Emergence of Cosmological Structures" of the Chinese Academy of Sciences (Grant No. XDB09000000). C. Wang acknowledeges the support from the National Natural Science Foundation of China (11273029).

Facility: Subaru (FOCAS)

REFERENCES

Beloborodov, A. M., & Thompson, C. 2007, ApJ, 657, 967
Cheng, A. F., & Ruderman, M. A. 1979, ApJ, 229, 348
Cheng, F. H., Shields, G. A., Lin, D. N. C., & Pringle, J. E. 1988, ApJ, 328, 223
Durant, M., & van Kerkwijk, M. H. 2006a, ApJ, 650, 1070
—. 2006b, ApJ, 650, 1082
Eichler, D., Gedalin, M., & Lyubarsky, Y. 2002, ApJ, 578, L121
García, L., & Gómez, M. 2015, Rev. Mexicana Astron. Astrofis., 51, 3
Gonzalez, M. E., Dib, R., Kaspi, V. M., Woods, P. M., Tam, C. R., & Gavriil, F. P. 2010, ApJ, 716, 1345
Gould, D. M., & Lyne, A. G. 1998, MNRAS, 301, 235
Han, J. L., Demorest, P. B., van Straten, W., & Lyne, A. G. 2009, ApJS, 181, 557
Hulleman, F., van Kerkwijk, M. H., & Kulkarni, S. R. 2000, Nature, 408, 689
Hulleman, F., van Kerkwijk, M. H., & Kulkarni, S. R. 2004, A&A, 416, 1037
Hurley, K., Cline, T., Mazets, E., et al. 1999, Nature, 397, 41
Kashikawa, N., et al. 2002, PASJ, 54, 819
Kaspi, V. M. 2007, Ap&SS, 308, 1
Kawabata, K. S., Okazaki, A., Akitaya, H., et al. 1999, PASP, 111, 898
Kern, B., & Martin, C. 2002, Nature, 417, 527
Kern, B., Martin, C., Mazin, B., & Halpern, J. P. 2003, ApJ, 597, 1049
Lundqvist, N., Lundqvist, P., Björnsson, C.-I., Olofsson, G., Pires, S., Shibanov, Y. A., & Zyuzin, D. A. 2011, MNRAS, 413, 611
Makishima, K., Enoto, T., Hiraga, J. S., et al. 2014, Physical Review Letters, 112, 171102
Malheiro, M., Rueda, J. A., & Ruffini, R. 2012, PASJ, 64, 56
Mereghetti, S. 2013, Brazilian Journal of Physics, 43, 356
Middleditch, J., Pennypacker, C. R., & Burns, M. S. 1987, ApJ, 315, 142
Mignani, R. P., Bagnulo, S., Dyks, J., Lo Curto, G., & Słowikowska, A. 2007, A&A, 467, 1157
Mignani, R. P., Moran, P., Shearer, A, Testa, V., Slowikowska, A., Rudak, B., Krzeszowki, K., & Kanbach, G. 2015, A&A, arXiv:1510.01057
Moran, P., Shearer, A., Mignani, R. P., Słowikowska, A., De Luca, A., Gouiffès, C., & Laurent, P. 2013, MNRAS, 433, 2564
Moran, P., Mignani, R. P., & Shearer, A. 2014, MNRAS, 445, 835
Morini, M., Robba, N. R., Smith, A., & van der Klis, M. 1988, ApJ, 333, 777
Olausen, S. A., & Kaspi, V. M. 2014, ApJS, 212, 6
Paczynski, B 1990, ApJ, 365, L9
Rea, N., et al. 2010, Science, 330, 944
—. 2012, ApJ, 754, 27
Rueda, J. A., Boshkayev, K., Izzo, L., et al. 2013, ApJ, 772, L24
Schmidt, G. D., Elston, R., & Lupie, O. L. 1992, AJ, 104, 1563
Słowikowska, A., Kanbach, G., Kramer, M., & Stefanescu, A. 2009, MNRAS, 397, 103
Tanaka, Y. T., Terasawa, T., Kawai, N., et al. 2007, ApJ, 665, L55
Tendulkar, S. P., Hascöet, R., Yang, C., et al. 2015, ApJ, 808, 32
Terasawa, T., Tanaka, Y. T., Takei, Y., et al. 2005, Nature, 434, 1110
Wagner, S. J., & Seifert, W. 2000, in Astronomical Society of the Pacific Conference Series, Vol. 202, IAU Colloq. 177: Pulsar Astronomy - 2000 and Beyond, ed. M. Kramer, N. Wex, & R. Wielebinski, 315
Wang, C., Lai, D., & Han, J. 2010, MNRAS, 403, 569
Wang, Z. 2014, Planet. Space Sci., 100, 19
Wang, Z., Chakrabarty, D., & Kaplan, D. L. 2006, Nature, 440, 772
Wang, Z., Chakrabarty, D., & Kaplan, D. L. 2008, in American Institute of Physics Conference Series, Vol. 983, 40 Years of Pulsars: Millisecond Pulsars, Magnetars and More, ed. C. Bassa, Z. Wang, A. Cumming, & V. M. Kaspi, 274–276
Wang, Z., Tanaka, Y. T., & Zhong, J. 2012, PASJ, 64, L1
Weltevrede, P. & Johnston, S. 2008, MNRAS, 391, 1210
Woods, P. M., & Thompson, C. 2006, Soft gamma repeaters and anomalous X-ray pulsars: magnetar candidates, ed. W. H. G. Lewin & M. van der Klis, 547–586

TABLE 1
PSF FITTING PHOTOMETRY OF 4U 0142+61

Sub-image	$m_{\rm psf}$ (mag)	$\Delta m_{\rm cor}$ (mag)	$m_{r=10}$ (mag)
e-beam$_{0\overset{\circ}{.}0}$	26.809±0.071	0.250	26.559±0.071
o-beam$_{0\overset{\circ}{.}0}$	26.858±0.072	0.246	26.612±0.072
e-beam$_{45\overset{\circ}{.}0}$	26.780±0.073	0.255	26.525±0.073
o-beam$_{45\overset{\circ}{.}0}$	26.792±0.078	0.256	26.536±0.078
e-beam$_{22\overset{\circ}{.}5}$	26.693±0.065	0.257	26.436±0.065
o-beam$_{22\overset{\circ}{.}5}$	26.846±0.081	0.253	26.593±0.081
e-beam$_{67\overset{\circ}{.}5}$	26.731±0.060	0.260	26.471±0.060
o-beam$_{67\overset{\circ}{.}5}$	26.874±0.076	0.255	26.619±0.076

Note: instrumental magnitude $m = 28 - 2.5\log(\text{flux})$; $m_{\rm psf}$, $\Delta m_{\rm cor}$, and $m_{r=10}$ are magnitudes obtained from PSF fitting, aperture corrections to a radius of 10 pixels (the uncertainties are negligible), and corrected magnitudes.